David Tomás Sánchez Martínez
Lourdes García Rodríguez
(coordinadores)

Proceedings of the 7th International Seminar on ORC Power Systems

Editorial Universidad de Sevilla

Proceedings of the 7th International Seminar on

ORC

Power Systems

David Tomás Sánchez Martínez
Lourdes García Rodríguez
(coordinadores)

Proceedings of the 7th International Seminar on

ORC Power Systems

(ORC2023)

4th to 6th
SEPTEMBER
SEVILLE 2023

EDITORIAL UNIVERSIDAD DE SEVILLA

Sevilla, 2024

Colección Actas
Núm.: 91

Review chairs of the 7th International Seminar on ORC Power Systems

Prof. Christoph Wieland (University of Duisburg-Essen) - *Review Chair*
Prof. Sotirios Karellas (National Technical University of Athens) - *Review Co-Chair*
Prof. Teemu Turunen-Saaresti (LUT University) - *Review Co-Chair*
Dr. Diego-César Alarcón-Padilla (Plataforma Solar de Almería - CIEMAT) - *Review Co-Chair*
Dr. Francesco Crespi (Universidad de Sevilla) - *Review Co-Chair*

c/ Porvenir, 27 - 41013 Sevilla.
Tlfs.: 954 487 447; 954 487 451; Fax: 954 487 443
Correo electrónico: info-eus@us.es
Web: https://editorial.us.es

ISBN 978-84-472-2745-7
DOI: https://dx.doi.org/10.12795/9788447227457

Diseño de cubierta y maquetación: los autores

INDEX OF CONTRIBUTIONS

SEVILLE 2023
7th International Seminar on O.R.C. Power Systems

DOI: https://dx.doi.org/10.12795/9788447227457_119

Simulation and Operation of a CSP that works with a HRB cycle

Antonio J. Subires[1*], Antonio Rovira[1]

[1]Universidad Nacional de Educación a Distancia (UNED), c/ Juan del Rosal, 12, 28040 Madrid, Spain,
*asubires@ind.uned.es

ABSTRACT

A Hybrid Rankine Brayton power cycle (HRB) is proposed as an alternative to the current technology used in Concentrated Solar Powerplants (CSPs) that work with medium temperatures (<400ºC). Other alternative power cycles that are common in the technical literature are presented in this paper for comparison purposes: a supercritical CO2 recompression Brayton cycle (sCO2-RB), and an Organic Rankine Cycle (ORC). To do this, a parametric analysis is first carried out to compare the efficiencies of the cycles. After that, the HRB power block with the highest efficiency is sized, and a new parametric analysis of the cycles is carried out taking the HRB design as reference. For this, the related parameters to the total area of the heat exchangers of the power block and the area of the solar field are standardized. After that, the designs that maximize the power produced for each cycle are selected. Finally, an annual simulation and a comparison between the annual energy produced for each case is done.

1 INTRODUCTION

1.1 Background

CSPs are a technology that plays a significant role in the electricity production through renewable energy. CSPs allow a dispatchable production, a characteristic that not all the renewable energy technologies have. This allows the decoupling between the availability of the renewable resource and the moment of electricity production. Consequently, production can be adjusted to the supply and demand curves. This is achieved by adding a heat storage system (TES) between the solar field and the power cycle.

The technology used in each of the CSP systems is quite established. For the solar field there are different solutions depending on the radiation concentration factor: Fresnel and parabolic trough collectors (PTC) for low-medium concentration and tower for high concentration. The higher the concentration, the temperature of the hot sink increases, leading to higher power cycle efficiencies. The technology mostly used in TES is the molten salt tanks, which exchange sensible heat with the heat transfer fluid (HTF) that comes from the solar field. For this, a hot and a cold storage tank are used, circulating the salts from one to the other depending on whether energy is stored or released from the system.

The steam Rankine power cycle with superheating, reheating and regenerative preheat is the most widespread choice. Different alternatives of power cycles as well as working fluids have been proposed in the technical literature. One of the main drawbacks of the Rankine steam cycle is the great complexity of the installation, since it includes many heat exchangers as well as steam extractions in the turbine. In the technical literature there are several studies that use subcritical and transcritical ORC alternatives[1], [2]. These cycles simplify the installation but are slightly less efficient than Rankine steam cycles. In ORCs, the steam extractions from the turbine are avoided and the number of recuperators is reduced (generally to just one). In addition, by choosing a suitable fluid, dry expansions are achieved in the last stages of the turbine as well as a high values of power density. ORCs applications are focused on the electricity production of limited power, through biomass, solar, geothermal, and waste heat from industrial processes [3], [4]. The main disadvantage of ORCs is the limitation of the maximum temperature they can reach (usually below 400ºC), so they are useful for medium and low temperature applications.

Another alternative is the sCO2-RB [5]. Although thermodynamic properties of CO2 are less attractive than those of the organic fluids usually used in ORCs, CO2 has no maximum temperature limitation, so it is recommended in high temperature applications (>500ºC). For turbine inlet temperatures higher than 550 °C, the sCO2-RB reaches higher efficiency values than the supercritical steam Rankine cycle [6].

The HRB configuration was presented in [7] . It includes some insights of the sCO2-RB that make it suitable for medium-low temperatures (<400ºC), obtaining higher efficiencies than the ORCs. However, the working fluid must be selected carefully to make it suitable for the cycle.

In this paper, four alternative power cycles (HRB propane, HRB isobutane, ORC toluene and sCO2-RB) are proposed to work in a 100 MW CSP with TES and PTC. The powerplant is located in Sevilla. In Section 1.2, a set of thermodynamic factors that allow to compare the efficiency of the power cycles are showed. In Section 1.3 and Section 1.4, the layout and general considerations of the cycles are described. Section 2 shows the methodology used to carry out the parametric analysis, the sizing of the different systems and the operation and simulation of a typical year. Section 3 shows the results and Section 4 the conclusions and future work.

1.2 Thermodynamic factors

Considering the Carnot efficiency, a set of factors are defined [8] .These factors allow to compare the efficiency of the different power cycles. Equation 1 shows that factors:

$$\eta = 1 - \frac{Q_c}{Q_h} = 1 - \frac{\tilde{T}_c \cdot \Delta s_c}{\tilde{T}_h \cdot \Delta s_h} = 1 - \frac{T_{min}}{T_{max}} \cdot \frac{T_{max}}{\tilde{T}_h} \cdot \frac{\tilde{T}_c}{T_{min}} \cdot \frac{\Delta s_c}{\Delta s_h} = 1 - \frac{1}{CN} \cdot \frac{1}{F_h \cdot F_C \cdot F_s} \quad (1)$$

Where $\tilde{T}_h$ is the mean temperature of heat addition, $\tilde{T}_c$ the mean temperature of heat rejection, Δs_h the entropy increment of heat addition and Δs_c the entropy increment of heat rejection. CN is the Carnot factor, which reduces the efficiency when the maximum and minimum temperatures of the cycle are closer. F_h and F_c are the factors of heat addition and rejection. These factors take the unit value when during the heat addition or rejection the temperature of the fluid is constant. This happens when processes take place through a latent heat exchange. Sensible heat exchanges take values lower than one. On the other side F_s is the entropy generation factor. This parameter considers the irreversibilities in all the processes of the cycle. 702

1.3 Description of the HRB cycle

In the HRB cycle, a Brayton and a supercritical Rankine cycle take place. Hybridization is achieved by bypassing part of the low-pressure flow that leaves the recuperator through a compressor as it is shown in Figure 1. Most of the main flow follows a supercritical Rankine cycle, while the bypass fraction follows a Brayton cycle.

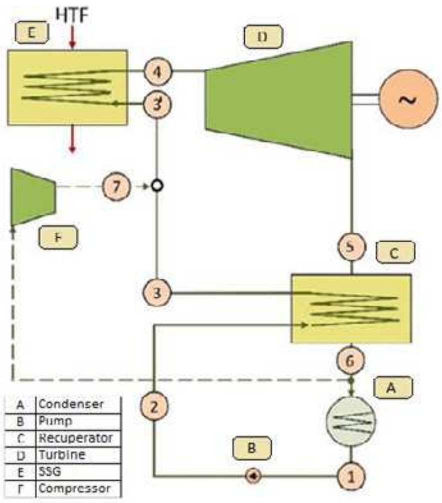

Figure 1: Layout of HRB cycle

F_c is high since the cooling process of the Rankine cycle is a condensing process. F_h is also high because the cycle includes a regenerator. The penalisation of F_s in the efficiency can be reduced selecting a good design: Choosing an optimal compression ratio can move the heat addition process away from the critical point, so the specific heat of the fluid remains constant during all the process. On the other hand, the irreversibility of mixing the bypassing flow and the flow that is heated in the recuperator could be reduced if the thermal properties are similar. Finally, selecting a proper bypassing factor could balance the heat capacity of the vapor and liquid state flows that exchanges energy in the recuperator.

It is important to choose a suitable working fluid. A high cp/R at ideal gas condition implies a lower difference between the specific heat of the vapor and the liquid state, so a lower recompression fraction value to balance the recuperator is needed. This leads to a lower compression work. Besides, it should be noted that a too high cp/R value can lead to wet compression, since the slope of the saturated vapor curve is positive. The proposed fluids, propane and isobutane, meet the above conditions. Figure 2 shows the T-S diagram of propane and isobutane cycles. It can be seen how the slope of the saturated vapor curve in isobutane is higher than that of propane.

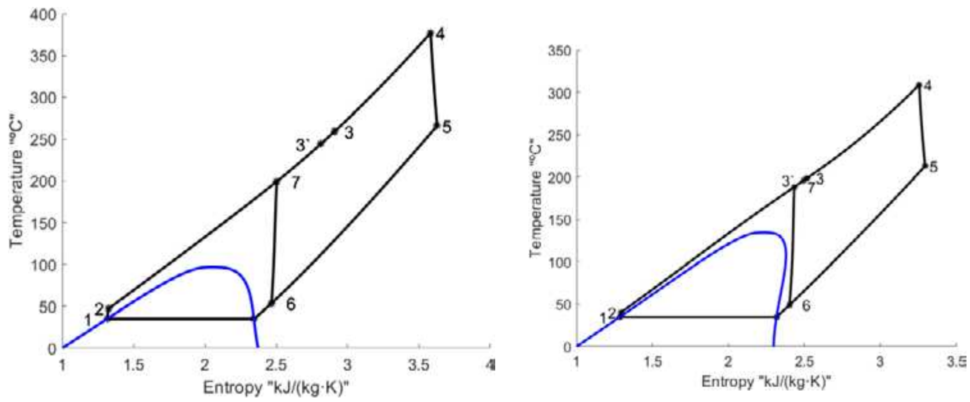

Figure 2: T-S diagram of HRB layout working with propane (left) and isobutane (right)

1.4 Description of sCO2-RB and ORC

sCO2-RB has a similar layout that the HRB but only changing the pump for a compressor, and the condenser for a cooler since the heat rejection is a sensible heat exchange. In this paper, the sCO2-RB showed has only one recuperator since the temperature range is not high. sCO2-RB in high temperature applications has two recuperators. The inlet compressor temperature and pressure is slightly above the critical point. The high specific heat capacity and low compressibility factor near this region, leads to a lower work of the compressor and a lower heat rejection mean temperature that increases the F_s factor. Figure 3 shows the T-S diagram of sCO2-RB cycle.

ORCs have different layouts depending on whether they are subcritical or transcritical. In the transcritical ones, the conventional boiling process is replaced by a sensible heating one that could lead to lower irreversibilities. As the recuperator is not balanced (there is not a bypass fraction), it is interesting select fluids with high heat capacity of the vapor to reduce the F_s. Toluene is a good candidate since it also has a high critical temperature. Figure 4 shows the T-S diagram of a transcritical and subcritical ORC toluene, respectively.

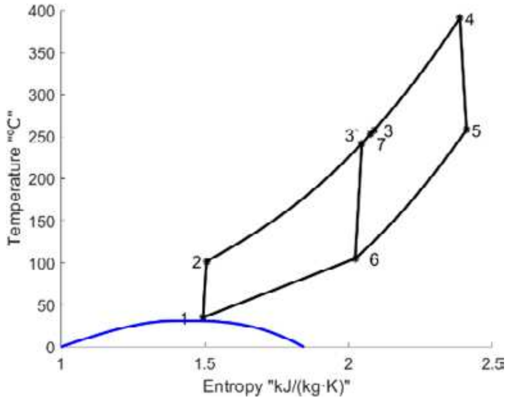

Figure 3: T-S diagram of sCO2-RB

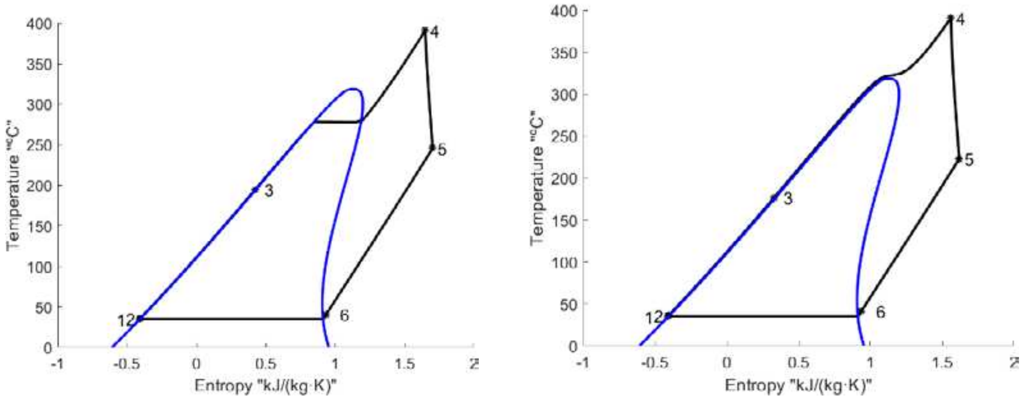

Figure 4: ORC toluene transcritical (left) and subcritical (right)

704

2 METHODOLOGY

2.1 Non standardized parametric analysis (NSPA)

The NSPA allows to compare the nominal efficiency of the different cycles from a set of fix and variable data. For each cycle, a map of efficiency values is obtained by varying the compression ratio (rc) and the bypass fraction, (x). The maximum rc value is limited by two conditions: A limit value of 300 bar in the high side pressure and a rc limit value of 20:1 for the turbocompressor. Besides, the inlet turbine temperature is limited by two conditions: The maximum temperature that the power fluid can reach without degradation (Table 1) and a minimum value of 5º in the SSG (HTF/propane heat exchanger) Pinch Point. The HTF inlet temperature in the SSG is considered equal to the solar field outlet temperature (396ºC).

The nominal dry bulb temperature considered is 25ºC and the temperature difference between the inlet air and the outlet power fluid is 10ºC, so the low temperature of the cycles is 35ºC. The sCO2-RB low pressure has been selected near the critical pressure to increase the density of the fluid at the compressor inlet. These input data are showed in Table 2.

The polytropic efficiency is used to calculate the inlet and outlet states related to the turbomachinery. To apply it, the enthalpy change in each turbomachinery is divided in 25 parts. For the pump and the compressor, Equation 2 is applied to each part. Equation 3 is used for the turbine. The SSG pressure drop corresponds to the high-pressure side and the recuperator SSG pressure drop corresponds to the low-pressure side. The pressure is assumed to decrease linearly.

Table 1: Maximum temperature limit of each fluid

	HRB Isobutane	HRB Propane	ORC Toluene	sCO2-RB
Maximum temperature limit (°C)	308.85	377	426.85	-

Table 2: Input data in the NSPA

	HRB Isobutane	HRB Propane	ORC Toluene	sCO2-RB
Fix data				
T_1(°C)	35	35	35	35
T_4(°C)	308.85	377	391	391
P_{cond} (bar) at 35°C	4.64	12.17	0.06	-
P_1 (bar)	4.64	12.17	0.06	80
SSG pressure drop	2%	2%	2%	2%
Recuperator pressure drop	5%	5%	5%	5%
Turbomachinery polytropic efficiency	0.9	0.9	0.9	0.9
Recuperator Pinch Point	5°	5°	5°	5°
Variable data				
x	0-0.27	0-0.25	-	0-0.29
rc	6-20	6-20	200-900	2.35-2.75

$$\eta_{pB,C} = \frac{dh_s}{dh} \quad (2) \qquad\qquad \eta_{pT} = \frac{dh}{dh_s} \quad (3)$$

The specific heat of the propane varies significantly around the critical point, so the Pinch Point in the recuperator can be achieved at the ends or inside it. So, the enthalpy change has been divided into 25 parts. This number is also enough to consider parallel flow heat exchangers without making significant errors. The next steps were taken to calculate the thermodynamic properties related to each part: 1º) T_3 is estimated. 2º) Energy balances are done in each segment, calculating the related temperatures. 3º) Pinch Point is calculated. 4º) A new T_3 is calculated using Newton-Raphson method. The process ends when the convergence is achieved. 705

2.2 HRB propane power block sizing

The power generated by the power block is 100 MW. Compression ratio and bypass fraction values are calculated in the NSPA and leads to the maximum power block efficiency. The nominal inlet and outlet temperature of the solar field are respectively 290ºC and 396ºC. The other fix input values are the same as the NSPA input values. The thermodynamic properties of each state are calculated like in the NSPA. The Recuperator UA factor is calculated by adding the UA factors of each part. The UA factor of each part is calculated from the heat exchanged ($\dot{Q}_i$) and the arithmetic mean temperature difference (AMTD_i) as it is showed in Equation 4. The SSG enthalpy change has been divided in 25 parts too. The SSG UA factor has been calculated with the same expression.

$$UA = \sum_{i=1}^{25} UA_i = \sum_{i=1}^{25} \frac{\dot{Q}_i}{\mathrm{AMTD}_i} \quad (4)$$

2.3 HRB propane cooling system sizing

The cooling system uses air, so the power consumption is significantly. The air mass flow rate ($\dot{m}_a$), can be calculated through the heat rejected ($\dot{Q}$), the specific heat capacity (cp_{air}), the Cooler Initial Temperature difference (ΔT_{ITD}) and the Cooler Approach temperature (AP_{cond}) as it is shown in Equation 5. The cooling UA factor is calculated as the sum of the UA factors associated to the rejection of sensible and latent heat of the cycle. In this case, the UA factors are calculated using the logarithm mean temperature difference (LMTD) since the refrigerator is not divided into smaller parts. The fan power is calculated as in [9].The fan power is proportional to the enthalpy increase of the air. The outlet fan temperature ($T_{fan,out,s}$) is calculated considering an isentropic compression (Equation 6) using the ideal gas model. The isentropic efficiency allows the calculation of the outlet enthalpy considering the irreversibilities. Finally, the fan power is calculated from the mechanical efficiency, the air mass flow rate, and the enthalpy increase. Table 3 shows the nominal data inputs.

$$\dot{m}_a = \frac{\dot{Q}}{cp_{air} \cdot (\Delta T_{ITD} - AP_{cond})} \quad (5)$$

$$T_{fan,out,s} = T_{db} \cdot rp_F^{\frac{R}{cp_{air}}} \quad (6)$$

Table 3: Cooling system input data

Fan isentropic efficiency	0.8
Fan mechanical efficiency	0.94
Cooler Initial Temperature difference*	10º
Cooler Approach temperature**	3º
Fan pressure ratio	1.0028

*It is defined as the difference between the outlet temperature of the power cycle and the air inlet temperature.
*It is defined as the difference between the condensing temperature of the power cycle and the air outlet temperature

2.4 Standardized parametric analysis (SPA)

The NSPA does not allow an adequate comparison between the cycles as it does not standardize the area of the heat exchangers (recuperator, SSG and refrigerator) nor solar field area. The SPA allows to compare the PB efficiency and the net power of the different cycles taking the sized HRB power block as reference. The calculated total UA factor of the heat exchangers (the sum of recuperator, SSG and refrigerator UA factors), the nominal inlet and outlet solar field temperatures, and the calculated nominal thermal power transmitted to the PB are the input data along with the data of Table 2 (except the recuperator Pinch Point, that is an output data). 706

Each power cycle is sized for each value of compression ratio and bypass fraction. The algorithm follows an iterative process in which each UA factor is initially estimated and then recalculated until convergence is achieved. The calculation of the thermodynamic properties related to the enthalpy change of each heat exchanger is calculated using the Newton Raphson method explained in Section 2.1 but considering the UA factor as a function instead off the Pinch Point.

For the HRB isobutane and ORC toluene cycles, the cooling UA factor is recalculated as it is showed in Section 2.3. In these two cases, the input data used are the same as those shown in Table 3. In the sCO2-RB, the UA factor is calculated by dividing the enthalpy change in 25 parts since the specific heat capacity of the CO2 varies significantly near the critical point. In this case, as the cooling process is a sensible heat exchange process, the outlet temperature of the air can be higher than the outlet temperature of the power fluid. So, in this case we consider that the temperature change value of the air is 20ºC.

2.5 Solar field sizing

The peak optical efficiency is calculated using Equation 7. The mirror reflectance (β), the intercept factor (γ), the envelope transmittance (τ) and the absorber absorptance (α) corresponds to geometrical and optical parameters of the collectors (Eurotrough-150) and the receivers (Schott PTR70).

$$\eta_{opt}|_{peak} = \beta \cdot \gamma \cdot \tau \cdot \alpha|_{\varphi=0º} \quad (7)$$

The incidence angle, φ, is calculated using the equation exposed in [10], [11] considering that the collectors rotation axis coincides with the North-South axis. Equation 8 allows to calculate the incidence angle modifier for an ET-150. This expression includes the cosine effect.

$$K = \cos(\varphi) - 2.859621e - 5 \cdot (\varphi)^2 - 5.25097e - 4 \cdot \varphi \quad (8)$$

The Equation 9 is used to calculate the heat losses per meter of absorber tube. ΔT is the difference between the average temperature of a collector loop and the dry bulb temperature.

$$\dot{q}_{perd} = 0.00154 \cdot \Delta T^2 + 0.2021 \cdot \Delta T - 24.89 + \left[(0.00036 \cdot \Delta T^2 + 0.2029 \cdot \Delta T + 24.899) \cdot \left(\frac{DNI}{900}\right) \cdot \cos(\varphi)\right] \quad (9)$$

The number of required Solar Collector Assemblies (SCAs) per loop is calculated using an energy balance (Equation 10). This value must be an even number since a collector loop is divided into two halves. Then, the HTF mass flow rate per loop ($\dot{m}_{col}$) is recalculated. h_{sfout} and h_{sfin} are the nominal outlet and inlet solar field enthalpies, A_{SCA} and L_{SCA} are the area and length of each SCA.

$$N_{SCA} = \dot{m}_{col} \cdot \frac{h_{sf_{out}} - h_{sf_{in}}}{DNI \cdot A_{SCA} \cdot \eta_{opt}|_{peak} \cdot K - \dot{q}_{perd} \cdot L_{SCA}} \quad (10)$$

The number of loops should be the upper integer number resulting from dividing the required thermal power by the thermal power of the unitary loop. As the solar multiple value is 2, the required thermal power is twice the thermal power demanded by the power block. The nominal input data is showed as Supplementary data.

2.6 Storage system sizing

Two-tanks system with a storage capacity for 12 hours of nominal power block thermal power requirement have been considered. The nominal temperatures of the hot and cold molten salts tanks are respectively 391ºC and 285ºC. The HTF/molten salts heat exchanger UA factor is calculated by the NTU method (Equation 11).

707

$$UA = NTU \cdot Cmin = \frac{\epsilon}{1-\epsilon} \cdot \frac{\dot{Q}}{T_{hot_{salt}} - T_{cold_{salt}}}; \quad \epsilon = \frac{T_{hot_{HTF}} - T_{cold_{HTF}}}{T_{hot_{HTF}} - T_{cold_{salt}}} \quad (11)$$

2.7 Off design power cycle/cooler calculation

The methodology assumes the following criteria: 1) The Stodola-Frügel Law is used to describe the behaviour of the steam turbine at partial load [12]. 2) We consider constant volumetric flow in the compressor. 3) The turbomachinery efficiency at off-design conditions is reduced from the nominal value as the capacity moves away from the design value. Equation 12 relates the turbomachinery efficiency to its capacity. Equation 13 describes the turbomachinery capacity from the mass flow rate, the pressure, and the inlet temperature. 4) The recuperator and SSG UA factors decrease as the mass flow rate of the fluid with the highest thermal resistance also does. The SSG UA factor is calculated using the Equation 14. The recuperator UA factor is also calculated using Equation 14 but considering propane instead of the HTF as fluid.

$$\eta_{tb} = \eta_{tb_{dis}} - \left|1 - \frac{\phi_{tb}}{\phi_{tb_{dis}}}\right| / 3 \quad (12) \qquad \phi = \dot{m}\frac{\sqrt{T}}{P} \quad (13) \qquad UA_{obj} = UA_{dis} \cdot \left(\frac{\dot{m}_{HTF}}{\dot{m}_{HTF_{dis}}}\right)^{0.8} \quad (14)$$

The off-design power cycle algorithm follows an iterative process in which the data input is the HTF temperature at the SSG inlet, the HTF mass flow rate, the cooling temperature, the inlet turbine temperature, and the low-pressure value. The main results are the thermal power required, the power production and the HTF temperature at the SSG outlet. T_6, P_4 and the bypass fraction are initially estimated and recalculated until they reach the convergence.

The off-design power cooler algorithm follows an iterative process in which the data input is the outlet and inlet cooler temperature at the power fluid side and the inlet temperature of the air. The main result is the power consumed by the fan. The outlet temperature of the air is initially estimated and recalculated until it reaches the convergence. Fan isentropic/mechanical efficiency and fan pressure ratio take the design value. Cooling UA factor is calculated using Equation 14 but considering the air instead of the HTF as fluid.

2.8 Annual simulations

The following operation conditions are considered in all cases: 1) The HTF mass flow rate through the SSG and the outlet temperature of the solar field take the design value; 2) Ambient temperature and inlet SSG temperature at HTF side (in the case that the TES provides thermal energy to the PB) take off-design values; 3) In HRB and the ORC, the low temperature is fixed 10ºC over the dry bulb temperature. 4) In the sCO2-RB, the low temperature is set in 35ºC. If the ambient temperature is higher than the design value, the air mass flow rate increases until a 15% higher than the nominal value.

The CSP follows a dispatch strategy that prioritizes production from energy coming directly from the solar field with only one PB startup per day. The PB startup is constrained by a time duration and a thermal energy fraction. The time duration constrain value is 30 min and the energy constraint value is a 20% of the thermal energy demanded by the PB during 1 hour at nominal conditions. The following premises are considered: 1) Every day after the solar field startup and before the PB startup, the minimum energy necessary to store is calculated so that the PB works uninterruptedly during daylight hours. 2) The PB startup operation only demands energy that comes directly from the solar field so the operation can take a longer time than the time duration constrain. 3) If the power absorbed by the solar field is higher than the maximum power that the cycle can demand, the power excess is derived to the storage system. 4) If the solar power absorbed is lower, the stored energy is transferred to the PB complementing the flow that comes from the solar field. 5) After the sunset, the salts are discharged at the nominal value, so the remaining energy stored is transferred to the PB increasing the production.

For each case we have done hourly simulations. The meteorological data used to calculate the annual simulations, correspond to a database of a typical year for Sevilla provided by METEONORM. It includes the weather station coordinates, as well as values taken hourly of DNI and dry bulb temperature. Row shadowing losses, solar field startup thermal energy and thermal tank losses are also considered. They are explained in [13], [14]. 708

3 RESULTS

Figure 5 shows the values of the efficiency for each cycle depending on the bypass fraction and the compression ratio in the NSPA. The highest efficiency value is achieved by the HRB propane cycle as it is showed in Table 4**.** Toluene achieve a slightly lower value. The compression ratio that corresponds with this value leads to a transcritical Rankine cycle. The F_s of ORC with toluene is high considering that the recuperator is not balanced. This occurs because the toluene has a high cp/R, so the vapor flow has a high specific heat. F_c of the sCO2-RB is considerable high although the heat rejected is sensible heat. This is because the inlet compressor flow is close to the critical point.

The HRB that works with isobutane has a higher value of F_s, F_c and F_h than the HRB that works with propane; however, the propane achieves a higher efficiency. This is because the isobutane has a lower maximum temperature, which penalizes the CN factor. sCO2-RB does not achieve high efficiency, which justifies that it works better with higher temperatures.

Table 5 shows the UA factors in case of sizing the cycles standardizing only the solar field. The thermal power required by the PB in each case coincides with that demanded by the HRB propane in the design that achieves the greatest efficiency. Temperature difference at the ends (cold and hot) of each heat exchanger are also showed. The HRB cycles need the highest total UA factor values while the ORC needs the lowest. The main reason is that the recuperator needs a higher UA in the cycles that have a bypass fraction. In these cases, the heat capacity is equalized, so the temperature change in each end of the recuperator is similar. Besides, recuperator UA factor in HRB propane is considerably higher than in the sCO2-RB cycle although the temperature difference at the ends is similar. This is because the specific heat capacity varies a lot inside the recuperator, so the temperature difference in each part of the recuperator can varies considerably too. This justifies the division of the heat exchanger in smaller segments. Besides, HRB and ORC cycles needs a higher cooler UA factor than in the sCO2-RB although in the latter, the efficiency of the cycle is the lowest. This is because HRB and ORC reject mostly latent heat while the sCO2-RB rejects only sensible heat.

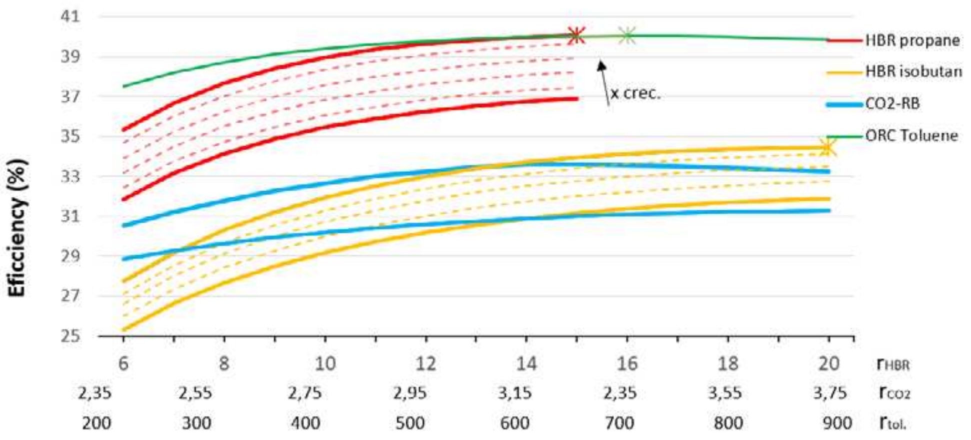

Figure 5: NSP results for each power cycle

Table 4. Maximum efficiency NSPA results for each power cycle

	HRB Isobutane	HRB Propane	ORC Toluene	sCO2-RB
Efficiency (%)	35.12	40.06	40.04	33.62
F_h	0.8956	0.8901	0.8446	0.8806
F_c	0.9989	0.9965	0.9998	0.9411
F_s	0.9123	0.8915	0.9163	0.8434
CN	1.889	2.109	2.155	2.155
x (bypass fraction)	0.25	0.25	-	0.29
rp (compression ratio)	20	15	700	3.15

Table 5: Standardized UA factors

	HRB Isobutane			HRB Propane			ORC Toluene			sCO2-RB		
	UA(MW/K)	ΔT_h	ΔT_c	UA	ΔT_h	ΔT_c	UA	ΔT_h	ΔT_c	UA	ΔT_h	ΔT_c
SSG	2.7	87	93	7.9	19	46	7.1	5	113	14.3	5	36
Recuperator	37.2	12	6	45.8	5.2	6.5	4.5	46	5	28.1	5	5
Cooler	38.2	21	3	22.3	20	3	25	16	3	6.5	73	10
Total	**78.1**	-	-	**75.9**	-	-	**36.6**	-	-	**48.9**	-	-

Table 6 shows the results of the SPA, that also standardizes the total UA factor. The design that maximizes the net power of each cycle is showed. All cycles increase their efficiency with respect to the SPA. ORC toluene produce more net power than the HRB propane as the UA total factor has been increased considerable. sCO2-RB produces more net power than the HRB isobutane although its efficiency is lower. As the cooler rejects only sensible heat in sCO2-RB, the temperature change of the cooler fluid (air) is higher, so the cooler power consumption is lower.

The results of the annual simulation for each power cycle are shown in Table 7. The thermal energy demanded by the PB is the solar thermal energy absorbed minus the solar field and PB startups and minus the heat losses in molten salts tank. In all cycles, these parameters are similar because the size of the TES and solar field are the same. The variations are due the heat losses by defocusing while the PB is off, and the TES is storing energy. Total net energy production in HRB Propane and ORC toluene are similar. The same happens between the HRB isobutane and sCO2-RB however in this case it is due the lower cooling system power consumption of the sCO2-RB. In all cycles, the average net power produced, and the average efficiency of the power block are slightly lower than the nominal values.

Table 6: Maximum efficiency SPA results for each power cycle

	HRB Isobutane	HRB Propane	ORC Toluene	sCO2 RB
Efficiency (%)	35.34	40.06	40.38	34.44
Power produced (MW)	88.5	100.3	101.1	86.2
Cooler consumption (MW)	7.3	6.8	6.7	2.6
Net Power produced(MW)	81.1	93.5	94.3	83.6
X (bypass fraction)	0.25	0.25	-	0.28
rp (compression ratio)	20	15	700	3.25
P_{max} (bar)	91.9	183	43.7	260
UA_{gv} (MW/K)	2.5	7.9	7.3	14.2
UA_{rc} (MW/K)	47.2	45.7	43.1	49.7
UA_{cond} (MW/K)	26.3	22.3	25.6	12.1

Table 7: Main Annual simulation results

	HRB isobutane	HRB Propane	ORC Toluene	sCO2-RB
Solar thermal energy absorbed (GWh)	1040.5	1039.5	1040	1036.8
Solar field startup thermal energy(GWh)	103.6	103.8	103.8	103.8
PB startup thermal energy(GWh)	16.8	16.8	16.8	16.8
Heat losses in molten salts tanks(GWh)	8.5	8.5	8.5	8.5
Thermal energy demanded by the PB (GWh)	911.5	910.4	910.9	907.6
Total energy production (GWh)	315.8	357.9	362	299.5
Cooling system consumption (GWh)	25.7	24.7	24.6	9.4
Total net energy production (GWh)	290	333.2	337.3	290
N° hours Power Block	3680	3672	3683	3720
Mean total power produced (MW)	85.8	97.5	98.3	80.5
Mean net power produced (MW)	78.8	90.7	91.6	80
Mean Power Block efficiency (%)	34.64	39.32	39.73	33
Power range (MW)	73.7/92	78.4/118.5	87.8/113.5	58/86.2
Net Power range (MW)	66.6/89	72.4/111.1	81/106	54.8/85
Cooling system power range (MW)	2.9/7.3	6/7.4	6.1/6.8	1.2/3
Power Block efficiency range (%)	31.25/36.07	34.34/42.19	35.61/42.61	25.53/34.44
Lower PB temperature range (°C)	30/55.5	17.7/53.2	17.7/53.2	35/44.5
Ambient temperature range (°C)	7.7/43.2	7.7/43.2	7.7/43.2	7.7/43.2

In all cases the net power range is wider than the power range because the cooling system consumes more energy at high ambient temperatures (when the PB efficiency is also lower). In HRB propane, the maximum power value is higher than in the ORC although the maximum efficiency value in the last is higher. This can be an advantage for the HRB when the objective is to produce more energy at the hours of highest sales price. Because of that the number of PB working hours is lower in the HRB propane than in the ORC. However, the minimum efficiency value in the HRB propane is considerably lower than the minimum efficiency value in ORC. This is because compressor and turbine rotate at same speed, so at high ambient temperature the bypass fraction value increases too much, unbalancing the recuperator and increasing the compressor consumption.

In HRB isobutane, the minimum condensing temperature is limited to 30ºC because lower temperatures could lead to wet compression. As a disadvantage, the maximum value of cycle efficiency in low ambient temperatures is also limited. However, the cooling power consumption is reduced. In sCO2-RB the minimum temperature of the cycle has been limited to 35 ºC. For ambient temperatures above the nominal, the cooling system has been optimized to work up to a maximum air flow of 1.15 the nominal value. With this, it has been possible to reduce the maximum value of the temperature at the compressor inlet to 44.5ºC when the ambient temperature is 43.2 ºC. Despite this, the performance is reduced up to a 25.53%. This is mainly due to the decrease in the density value at the compressor inlet.

4 CONCLUSIONS

Different power cycles have been presented as alternatives to the current technologies used in CSPs. A method that allows to compare the performance of the power cycles without sizing the solar field and the TES has been proposed. To achieve this, the UA factors of the PB and the thermal power demanded have been standardized. Annual simulations have been done to compare the annual energy production. In this case, the same solar field and TES have been sized for all the power cycles studied.

The low consumption of the sCO2-RB aerocondenser is an advantage, but the efficiency is severely penalized when the compressor inlet conditions are far from the critical point. On the other hand, despite the high efficiency developed by the ORC toluene, it has a major drawback: Condensing pressures for common ambient temperatures are very low, in vacuum. So, air can enter in the circuit. This is a risk considering that toluene is very flammable. The HRB propane cycle with a balanced recuperator has proven to develop high performance for medium temperature applications. The critical pressure of propane is not very high, which allows working in the supercritical region without too high pressures. Independent shafts for turbine and compressor could lead to select different bypassing fractions in each off-design condition. So, the performance could be increased considerably at high ambient temperatures.

Supplementary data: AntonioSubires/Supplementary-data-of-Simulation-and-Operation-of-a-CSP-that-works-with-a-HRB-cycle- · GitHub

711

ACKNOWLEDGMENTS

Grant PID2019-110283RB-C31 and PRE2020-094353 funded by MCIN/AEI/ 10.13039/501100011033, by “ESF Investing in your future” and, as appropriate, by “ERDF A way of making Europe”, by the “European Union” or by the “European Union NextGenerationEU/PRTR”.

REFERENCES

[1] H. Singh and R. S. Mishra, “Performance evaluation of the supercritical organic rankine cycle (SORC) integrated with large scale solar parabolic trough collector (SPTC) system: An exergy energy analysis,” *Environ Prog Sustain Energy*, vol. 37, no. 2, pp. 891–899, Mar. 2018, doi: 10.1002/ep.12735.

[2] D. Sánchez, B. M. Brenes, J. M. Muñoz de Escalona, and R. Chacartegui, “Non-conventional combined cycle for intermediate temperature systems,” *Int J Energy Res*, vol. 37, no. 5, pp. 403–411, Apr. 2013, doi: 10.1002/er.2945.

[3] E. Cayer, N. Galanis, and H. Nesreddine, “Parametric study and optimization of a transcritical power cycle using a low temperature source,” *Appl Energy*, vol. 87, no. 4, pp. 1349–1357, 2010, doi: 10.1016/j.apenergy.2009.08.031.

[4] B. F. Tchanche, G. Lambrinos, A. Frangoudakis, and G. Papadakis, “Low-grade heat conversion into power using organic Rankine cycles - A review of various applications,” *Renewable and Sustainable Energy Reviews*, vol. 15, no. 8. Elsevier Ltd, pp. 3963–3979, 2011. doi: 10.1016/j.rser.2011.07.024.

[5] Y. Liu, Y. Wang, and D. Huang, “Supercritical CO2 Brayton cycle: A state-of-the-art review,” *Energy*, vol. 189. Elsevier Ltd, Dec. 15, 2019. doi: 10.1016/j.energy.2019.115900.

[6] J. I. Linares, M. J. Montes, A. Cantizano, and C. Sánchez, “A novel supercritical CO2 recompression Brayton power cycle for power tower concentrating solar plants,” *Appl Energy*, vol. 263, Apr. 2020, doi: 10.1016/j.apenergy.2020.114644.

[7] A. Rovira, M. Muñoz, C. Sánchez, and J. M. Martínez-Val, "Proposal and study of a balanced hybrid Rankine-Brayton cycle for low-to-moderate temperature solar power plants," *Energy*, vol. 89, pp. 305–317, Sep. 2015, doi: 10.1016/j.energy.2015.05.128.

[8] A. Rovira, C. Rubbia, M. Valdés, and J. M. Martínez-Val, "Thermodynamic cycles optimised for medium enthalpy units of concentrating solar power," *Energy*, vol. 67, pp. 176–185, Apr. 2014, doi: 10.1016/j.energy.2014.02.029.

[9] M. J. Wagner and P. Gilman, "Technical Manual for the SAM Physical Trough Model," 2011.

[10] J. A. Duffie and W. A. Beckman, *Solar Engineering of Thermal Processes*, 2nd ed. New York: John Wiley & Sons, 1991.

[11] A. Rabl, *Active solar collectors and their applications*. New York : Oxford University Press, 1985.

[12] A. Rovira, R. Abbas, C. Sánchez, and M. Muñoz, "Proposal and analysis of an integrated solar combined cycle with partial recuperation," *Energy*, vol. 198, 2020, doi: 10.1016/j.energy.2020.117379.

[13] A. J. Subires and A. Rovira, "Economic Optimization of a Thermal Solar Power Plant that Operates with a HRB Cycle by Improving the Operation Schedule," in *SolarPACES 2022 – 26th International Conference on Concentrating Solar Power and Chemical Energy Systems* ,

[14] A. J. Subires and A. Rovira, "Sizing and simulation of a solar thermal power plant that operates with a HRB cycle," in *XII National and III International Conference on Engineering Thermodynamics (CNIT 2022).*, Madrid.

This book contains the compilation of works contributed to the *7th International Seminar on Organic Rankine Cycle Power Systems* (ORC 2023), held in Seville between the 4th and 6th of September 2023. The event was hosted by Universidad de Sevilla on behalf of the Knowledge Centre on Organic Rankine Cycle Technology (KCORC), incorporated in The Netherlands.

The ORC conference, organized biennially, stems as the only conference that is specific to ORC technology, therefore gathering a diverse community whose affiliation spans across all the interested stakeholders, not only in this particular technology but also and in a broader context, in the energy transition. Original equipment manufacturers, professional associations, end-users, investors, policy makers, academics, scientists feel at home at ORC 2023.

The almost 100 proceedings in this book cover a wide variety of topics, from fundamentals to system integration through component design, accounting for thermodynamic performance as well as component design. In addition to this, and as a new track in 2023, works on heat pump technology were also accepted in order to raise awareness of the strong ties between both technologies, specifically in energy storage applications.

This book provides an excellent overview of the current maturity of power systems based on Organic Rankine Cycle technology for applications as diverse as geothermal and waste heat recovery in industry or downstream of other prime movers (e.g., marine applications). It is also an excellent source of information to understand the current challenges faced by the technology, stemming from a very competitive market and increasingly stringent environmental regulations.

The organizers of ORC 2023 hope that the reader finds this work as exciting as the attendees to the conference and, maybe, make the decision to join the 8th edition to the conference in 2025.

KCORC
KNOWLEDGE CENTER
ORGANIC RANKINE CYCLE

eUS EDITORIAL
UNIVERSIDAD DE SEVILLA